

Adaptive Optimal Design of Active Thermally Insulated Windows Using Surrogate Modeling

Junqiang Zhang*, Achille Messac†, Souma Chowdhury* and Jie Zhang*

Rensselaer Polytechnic Institute, Troy, NY, 12180

This paper explores the adaptive optimal design of Active Thermally Insulated (ATI) windows to significantly improve energy efficiency. The ATI window design uses thermostats to actively control thermoelectric (TE) units and fans to regulate the overall thermodynamic properties of the windows. The windows are used to maintain a comfortable indoor temperature. Since weather conditions vary with different geographical locations and with time, the thermodynamic properties of the windows should adapt accordingly. The electric power supplied to the TE units and the fans are dynamically controlled so as to provide an optimal operation under varying weather conditions. Optimization of the ATI window design is a multiobjective problem. The problem minimizes both the heat transferred through the window and electric power consumption. The heat transfer through the ATI windows is analyzed using FLUENT; and the optimization is performed using MATLAB. Since the computational expense of optimization for numerous weather conditions is excessive, the power supplies are optimized under a reasonably small number of weather conditions. Based on the optimal results obtained for these conditions, a surrogate model is developed to represent the optimal results in a wide range of weather conditions. The surrogate model is used to evaluate optimal power supplies with respect to different values of outside temperature, wind speed, and intensity of solar radiation. Thermometers, anemometers, and solar radiation sensors are used to sense these weather conditions. With the inputs from the sensors, the thermostats determine the operating conditions and calculate the corresponding optimal power supplies using the surrogate model. Since the ATI windows are operated with optimal power supplies, high energy efficiency is achieved.

I. Introduction

Since global demand for energy is continuously growing, there is an ongoing critical search for new technologies that can reduce energy consumption to alleviate the deleterious effects on the environment, while promoting economic development. A technical report shows that 44% of energy consumed in commercial buildings is used for space heating and cooling in the US in 2003.¹ Improving the insulating properties of building envelopes can greatly reduce energy consumption. Research shows that windows or glass facades contribute significantly to the thermal imbalance in residential and commercial buildings. Windows, which occupy only 10% to 15% of the wall area, can contribute 25% to 30% of the heat exchange.^{2,3} Therefore, improvement to the thermal insulation of windows can significantly reduce energy consumption in buildings.

Advancement in window technology has been pursued in different ways; one is to actively respond to the ambient conditions by changing the thermodynamics of windows. These new window designs are called active windows and some are claimed to have the potential to reduce peak electrical loads by 20% to 30% in many commercial buildings.⁴ Examples of these active windows include active control of motorized shading systems,⁵ switchable window coatings,^{6,7} heat extraction double skin facades,⁴ airflow windows,^{8,9} and thermoelectric windows.¹⁰⁻¹³

In the thermoelectric window design, thermoelectric technology¹⁴ is integrated, and the design is optimized to maximize insulation. Thermoelectric (TE) units can provide effective heat transfer when supplied

*Doctoral Student, Department of Mechanical, Aerospace, and Nuclear Engineering, AIAA student member

†Professor, Department of Mechanical, Aerospace, and Nuclear Engineering, AIAA Lifetime Fellow. Corresponding author (messac@rpi.edu)

with electric power. The windows have multiple glass panes, and the TE units are installed on window frames between panes. TE units can transfer heat in the direction opposite to the passive heat flow through the glass panes (see Sec. II.A). Fans are used to enhance the performance of TE units. The windows have sensors and thermostats. Sensors are used to detect weather conditions and thermostats can control the directions and magnitudes of electric voltages of TE units.

Since weather conditions vary with geographical locations and with time, the optimal design for a certain location under one specific weather condition may not be optimal for other locations and other weather conditions. To achieve both low heat transfer through ATI windows and high energy efficiencies under changing weather conditions, the windows should have adaptive capabilities to adjust operating points. In optimal design process, adaptive optimization is used to maintain optimal performances of the ATI windows when weather conditions change during operation.

Because of abilities to offer high performance under changing operating conditions, adaptive optimization is applied on designs of aircrafts^{15,16}, robots,¹⁷ and engines.¹⁸ In ATI window designs, sensors are used to measure weather conditions, and thermostats are used to dynamically control the power supplied to TE units and fans. Since the weather conditions are varying, adaptive optimization is applied on the design to minimize power supplies and heat transferred through the windows under different weather conditions.

Modern product and system design typically requires extensive use of simulation-based and analysis tools, such as finite element analysis, computational fluid dynamics (CFD), and other computationally intensive models. In the ATI window design, a CFD model is created and used to simulate the heat transfer process between outdoor and indoor. Since the computational expense of the CFD model is high, the optimization is not performed for every different weather condition. It is performed for a reasonably small number of conditions, and the results are used to develop a surrogate model to represent optimal results under a wide range of weather conditions. The Response Surface Method is a popular technique used to create surrogate models,^{18,19} and it is used in the ATI window design.

This paper develops the design of ATI windows in Section II. The adaptive optimization of the design is formulated in Section III. In Section IV, how to adaptively achieve the optimal performances of ATI windows is presented. The performance of ATI windows is compared with standard passive windows in Section V. Concluding remarks are presented in section VI.

II. Active Thermally Insulated Windows

The ATI window design is an improvement upon existing multi-pane windows. To increase the insulation of windows, more panes are added to single-pane passive windows, leading to multi-pane windows. The ATI window integrates TE units, thermostats and sensors to actively control the overall thermodynamics of such multi-pane windows.

The ATI windows are used throughout the year. The indoor temperature is assumed kept at a comfortable value. Sometimes the indoor temperature is higher than the outdoor temperature, and at other times it is lower. In this paper, heating condition is defined as: when the indoor temperature is higher than the outdoor temperature, the ATI windows need to reduce the heat transferred from inside to outside. Cooling condition is defined as: the indoor temperature is lower than the outdoor temperature and the ATI windows need to reduce the heat transferred from outside to inside.

There are eight major subsystems in the ATI window: the air gap, the two side channels, the TE units, the two fins in the side channels, the heat sink, the fans, the sensors, and the thermostat. These components and their functions distinguish the ATI window from traditional passive windows.

A simplified schematic of the ATI window is shown in Fig. 1. The geometry and properties of the window is detailed in Table 1.

The ATI window has three panes as shown in the section view in Fig. 1(b). They are named the inner pane, the middle pane and the outer pane, respectively. The air gap between the middle and outer panes is not controlled, which is same as that in a traditional window. The thermodynamic properties of the air gap between the inner and middle panes are controlled so as to minimize the heat transfer through the inner pane. The TE units are located in the two side channels. Inside either of the left or the right side channel, there is a thin rectangular fin that is connected to the TE units to increase heat exchange between the TE units and the air flow through the channel. To reduce the thermal resistance between the outdoor environment and the TE units, heat sinks are connected to the side of TE units that interacts with the outside air. Fans are installed both on the top and the bottom of the air gap between the inner pane and the

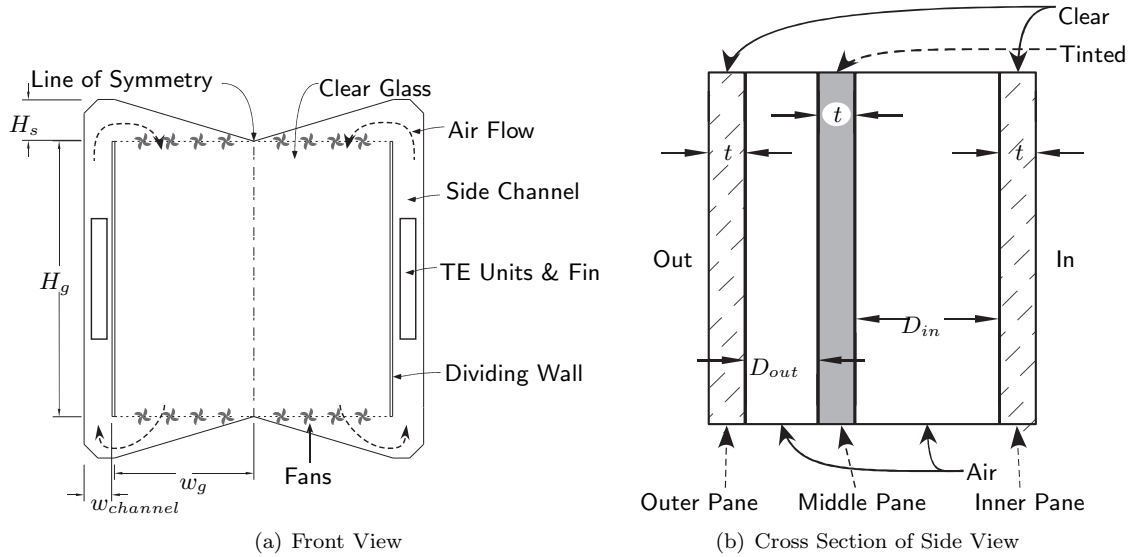


Figure 1. Schematic of the ATI Window

Table 1. ATI Window Geometry

Property	Symbol	Value	Units
Height of the glass	H_g	1.00	m
Half width of the glass	w_g	0.50	m
Height for the channel	H_s	0.15	m
Width of the channel	$w_{channel}$	0.10	m
Inner gap depth	D_{in}	0.024	m
Outer gap depth	D_{out}	0.012	m
Pane thickness	t	0.006	m

middle pane to assist the convection. The air flow goes through the side channels and is heated or cooled by the fins. Figure 1(a) illustrates the air flow under heating conditions. Under heating conditions, the air in the side channels is heated by the fins and rises to the top of the channels. After the air flows out of the channels, it encounters the cold glass of the air gap, cools, flows down to the bottom, and goes back into the side channels. As the air flows down, it warms the inner pane, and thereby reduces the heat lost from the room. Under cooling conditions, the air is cooled by the fins in the side channels, and it reduces the heat added to the room through the inner pane by cooling the inner pane.

ATI windows have sensors to detect weather conditions. The signals from the sensors are fed into a thermostat. The thermostat controls electric power supplied to the TE units and the fans. Under different weather conditions, the thermostat can adjust the power supplies to optimal operating conditions, which is discussed in Section II.F.

As Fig. 1(b) shows, the inner pane and the outer pane are clear glass and the middle pane is tinted. The tinted pane can absorb more solar energy than a clear glass pane. If the inner pane is tinted, the absorbed solar heat is beneficial under heating conditions. However, it is detrimental under cooling conditions. If the outer pane is tinted, it is insulated from the inside air and does not significantly benefit heating. To address the conflict, the tinted pane is installed in the middle and is insulated from both the indoor and outdoor environments.

II.A. Modeling TE Units

The ATI windows use TE units to control the heat transferred through the inner panes. Each TE unit consists of thermocouples which, when supplied with electric current, induce heat flow in the direction of the current. This is known as the Peltier effect.¹⁴ Because of the thermocouples' electrical resistance, heat

is generated - the Joules effect. As the results of the two conflicting effects, heat is absorbed on the cold side and released from the hot side. A temperature difference is created across the TE units. On the cold side of TE units, the heat rate is predicted as²⁰

$$Q_{cold} = 2N_{te}N \left[\alpha I_{te} T_c - \frac{I_{te}^2 \rho}{2G} - \kappa \Delta T_{te} G \right] \quad (1)$$

where N_{te} is the number of TE units; N is the number of thermocouples in each TE unit; α is the Seebeck coefficient; I_{te} is the electric current; T_c is the cold side temperature; ρ is the resistivity; G is the geometry factor, which represents the area to thickness ratio of the thermocouple; κ is the thermal conductivity; and ΔT_{te} is the temperature difference across the thermocouple. For a given TE unit, α , ρ , and κ are temperature dependent properties, N and G are constants, and are all provided by the manufacturer.²⁰

The voltage drop across the TE unit is given by²⁰

$$V_{te} = 2N \left[\frac{I_{te} \rho}{G} + \alpha \Delta T_{te} \right] \quad (2)$$

The heat released from the hot side of the TE unit is the combination of the heat absorbed by the TE and the heat generated by electric current, which is given by

$$Q_{hot} = N_{te} I_{te} V_{te} + Q_{cold} \quad (3)$$

The maximum allowable applied current, I_{max} , is given by²⁰

$$I_{max} = \frac{\kappa G}{\alpha} \left[\sqrt{(1 + 2ZT_h)} - 1 \right] \quad (4)$$

where Z is the figure-of-merit provided by the manufacturer, T_h is the hot side temperature, and the other variables are defined above.

The maximum allowable temperature difference, ΔT_{max} , is given by

$$\Delta T_{max} = T_h - \left[\frac{\sqrt{(1 + 2ZT_h)} - 1}{Z} \right] \quad (5)$$

The values of the TE properties are provided by the manufacturer and the values used in this study are listed in Table 2 (for 300 K).

Table 2. TE Units Properties for 300 K²⁰

Parameter	Symbol	Value	Units
Seebeck coefficient	α	2.00×10^{-4}	V/K
Resistivity	ρ	9.87×10^{-4}	Ωcm
Thermal conductivity	κ	1.54×10^{-2}	W/cm K
Figure of merit	Z	2.67×10^{-3}	1/K
G-Factor	G	0.076	cm^{-1}
Number of Thermocouples	N	71	

Since ATI windows are used in both heating and cooling conditions, they reduce the passive heat transfer either from inside to outside or in the opposite direction. One side of the TE unit is connected with the fin in the channel and interacts with the air flow in the channel, while the other side is connected with the heat sink installed on the outside surface of window frames, and is exposed to the outdoor environment. Note that heating condition and cooling condition can be reversed simply by reversing the polarities of the TE units, thereby causing the current to reverse direction. Consequently, the hot side and the cold side of the TE units also switch. In heating conditions, the cold side of the TE unit is exposed to outdoor environment and the hot side releases heat to the air flow in the side channels. While in cooling conditions, the hot side of the TE units is exposed to outdoor and the cold side absorbs heat from the air flow in the side channels. The side of the TE units exposed to the outdoor environment has a heat sink to enhance the heat transfer from the TE unit, which is discussed in Section II.C.

II.B. Side Channels and Air Gap

The fluid thermal simulation model of the side channels and the air gap is created using the computational fluid dynamics (CFD) software FLUENT. The model simulates the steady-state heat transfer process. The model only represents half of the system, and the other half is predicted using a symmetry condition. The outer pane, the middle pane, and the air gap between these two panes are modeled as one pane with a thermal resistance equivalent to the summation of the three. To account for the solar radiation absorbed by the outer pane and the middle pane, the FLUENT model considers it as volumetric heat generation in the equivalent pane.

In this study, the middle pane is assumed to be a generic bronze glass, and the other two panes are clear. From the analysis of the glazing system in *Window*²¹ program, the solar absorption of the inner pane is approximately only one tenth that of the other two and is neglected. The value for S_A , listed in Table 3, is the sum of the solar absorption coefficient of the outer and middle panes. The value for S_R is the reflectivity of the outer pane alone. The conductivity of the glass is also shown in Table 3.

Table 3. ATI Window Pane Properties

Property	Symbol	Value
Solar Absorption ²²	S_A	53%
Solar Reflection ²²	S_R	11%
Glass Conductivity ²²	k_g	0.84 W/m

In FLUENT, the discrete transfer radiation model is used to evaluate the radiative heat transfer.²³ The room temperature is taken as the radiative temperature inside the room. The radiative mean temperature of the sky is estimated by²⁴

$$T_{rm} = \left(\frac{[F_g + (1 - f_{clr}) F_s] \sigma T_{out}^4 + f_{clr} F_s J_s}{\sigma} \right)^{1/4} \quad (6)$$

where F_s and F_g are the view factors of the sky and ground, respectively; f_{clr} is the percentage of possible sunlight taken to be the average fraction of clear sky; σ is the Stefan-Boltzmann constant; T_{out} is the outside temperature; and J_{sky} is the radiation falling onto a horizontal surface. The relation between J_{sky} and T_{out} has been found to be²⁴

$$J_{sky} = (5.31 \times 10^{-13}) T_{out}^6 \quad (7)$$

The FLUENT model has 32010 nodes. The heat transfer process is steady-state. The air flow between the inner pane and the middle pane is laminar. A pressure based solver in FLUENT is used. The convergence criteria were set as: the residuals of velocities are less than 0.001m/s.

The inputs to the FLUENT model are the channel temperature, T_{chan} , and the fan pressure gradients. After the model is evaluated, the heat flux through the inner pane, and the heat flux through the fins inside channels, are returned as outputs.

Although the solar radiation absorbed by the panes is accounted for by CFD analysis, the solar energy that passes through the panes directly into the room is not accounted for. The solar radiation through the panes into the room is given by

$$Q_{solar} = E_{sky} (1 - S_A - S_R) \quad (8)$$

where E_{sky} is the solar radiation.

The total heat flux through the inner pane of the ATI window is given by

$$Q_{ATI} = Q_{CFD} + Q_{solar} \quad (9)$$

where Q_{CFD} is the heat flux into the room estimated by FLUENT.

II.C. Heat Sink Modeling

To reduce the thermal resistance between the outdoor environment and the TE units, heat sinks are connected to the side of TE units that interacts with the outside air. For this design, pinned heat sinks are used. The

pins have lower thermal resistance than rectangular fins and they also allow for either vertical natural convection or horizontal crosswinds. The thermal resistance of a pinned heat sink is given by²⁵

$$R_{hs} = \left(N \tanh(md) \sqrt{hpk_{pin}A_c} \right)^{-1} \quad (10)$$

where N is the number of pins; h is the convective heat transfer coefficient; p , k_{pin} , d , and A_c are the perimeter, thermal conductivity, depth, and cross sectional area of a single protrusion, respectively. The fin conductivity, k_{fin} , is taken to be that of aluminum, 164 W/cm K.²⁵ The fin property, m , is further defined as

$$m = \sqrt{\frac{hp}{kA_c}} \quad (11)$$

The heat transferred through the heat sink can be determined by

$$Q_{hs} = \frac{\Delta T_{hs}}{R_{hs}} \quad (12)$$

where ΔT_{hs} is the temperature difference between the TE unit and the outdoor environment.

Stanescu et al. interpolated the optimal spacing of pins in forced convection based on an experimental study.²⁶ A ratio of optimal spacing to the diameter is given by²⁶

$$\left(\frac{S}{D} \right)_{opt} \cong 2.2Pr^{-0.13} \left(\frac{D}{H} \right)^{-2/5} Re_D^{-3/10} \quad (13)$$

where S is the spacing, which is defined as zero when the cylinders are touching; Pr is the Prandtl number; D is the diameter of the pin; H is the height of the array; and Re_D is the Reynolds number based upon the diameter of the pin. The optimal fin spacing, S_{opt} , which maximizes the natural convection from the finned surface, is given as²⁶

$$S_{opt} = \left[\left(\frac{S}{D} \right)_{opt} + 1 \right] D \quad (14)$$

The lowest feasible value for the diameter of the pins is 2.57mm, which considers neither the prices of materials nor the cost of production.

II.D. Fan Modeling

In the ATI window design, sixteen fans are used to introduce forced convection on the air flow between the inner pane and the middle pane. As shown in Fig. 1(a), half of them are installed on the top of the air gap, and the other half are installed on the bottom. The pressure gradients produced by the fans are constrained to be very small. The forced convection resulted from the pressure gradients is not significant. Under heating conditions, the directions of the fan pressure gradients are opposite to cooling conditions, since the direction of the air flow is opposite.

Assuming no power losses, the ideal power consumption of a fan can be expressed as²⁷

$$P_{ideal} = \Delta p \times q \quad (15)$$

where P_{ideal} is the ideal power consumption; Δp is the pressure gradient produced by the fan; and q is the air volume flow delivered by the fan.

The total ideal electric power consumption of N fans is

$$P_{total} = \sum_{i=1}^{N_{fan}} P_{ideal}^i \quad (16)$$

The sixteen fans are separated into four groups according to their locations, the top left, the top right, the bottom left, and the bottom right (see Fig. 1(a)). It is assumed that, in each group, the pressure gradient of each pan is expressed by a linear function of an average pressure gradient and a slope. The average pressure gradient, Δp_{avg} , and the slope, k , are the same for four different groups. Inside each group, the four fans

Table 4. Pressure Gradients of Fans in Four Groups

Group	Left Most	Center Left	Center Right	Right Most
Top Left	$(1 - 3k)\Delta p_{avg}$	$(1 - k)\Delta p_{avg}$	$(1 + k)\Delta p_{avg}$	$(1 + 3k)\Delta p_{avg}$
Top Right	$(1 + 3k)\Delta p_{avg}$	$(1 + k)\Delta p_{avg}$	$(1 - k)\Delta p_{avg}$	$(1 - 3k)\Delta p_{avg}$
Bottom Left	$(1 - 3k)\Delta p_{avg}$	$(1 - k)\Delta p_{avg}$	$(1 + k)\Delta p_{avg}$	$(1 + 3k)\Delta p_{avg}$
Bottom Right	$(1 + 3k)\Delta p_{avg}$	$(1 + k)\Delta p_{avg}$	$(1 - k)\Delta p_{avg}$	$(1 - 3k)\Delta p_{avg}$

are named Left Most, Center Left, Center Right, Right Most. The left half and the right half of the window are symmetric. The pressure gradients of the fans are expressed in Table 4.

From the optimal results obtained in Section III, the total power consumption of fans, P_{total} , is less than 6% of TE units power consumption. Although one of the objective is to minimize electric power consumption, the power consumption of the fans is not set as an objective, since it is much smaller than that of the TE units.

II.E. Sensors

In the optimization, the objective is to minimize both the electric power consumption and the heat transfer through the inner pane. Under a given weather condition, one set of optimal values of electric powers is evaluated. If any parameter of the weather conditions, including the outside temperature, the wind speed, and the intensity of solar radiation, is changed, the optimal results will change. It is essential for the ATI windows to detect the weather conditions and adjust the power supplies to optimal values. Three kinds of sensors, thermometers, anemometers and solar radiation sensors, are used to measure outside temperatures, wind speeds, and the intensity of solar radiation, respectively. The signals, from thermometers, anemometers and solar radiation sensors, are input into thermostats, as presented in Section II.F.

II.F. Thermostats

Since ATI windows need to adjust the electric power supplies of TE units and fans according to different weather conditions, thermostats are used to control the electric voltages. Thermostats receive the signals from sensors and control the direction and magnitudes of electric voltages of the TE units and the fans, as shown in Fig. 2.

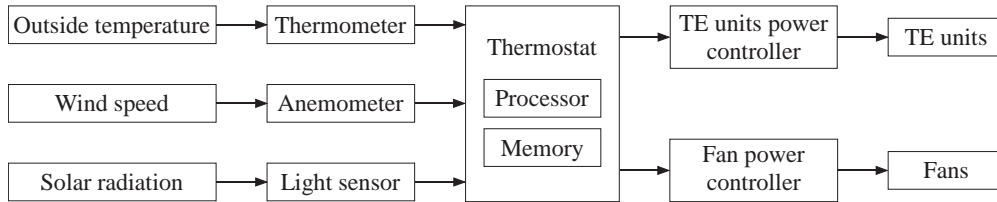


Figure 2. Thermostat and Sensors

With the utilization of digital technology, thermostats have processors and memories. Thermostats can process signals and control outputs. Three functions, which are derived in Section IV, are stored in the thermostats to calculate the electric voltages of the TE units and the fans to achieve optimal operations. Outside temperatures, wind speeds, and solar radiation are inputs from the sensors, and they are variables of the functions. The processor of the thermostat calculates the optimal electric voltages, and the thermostat adjusts the voltages to optimal values according to the specific weather condition.

Without thermostats, the power supplied to the TE units and the fans cannot change under varying weather conditions, and hence will not be always optimal. Thermostats actively change the overall thermodynamics of ATI windows by controlling the power supplies, and optimal performances can be maintained given different weather conditions within a reasonable range.

III. Adaptive Optimization of ATI Windows

III.A. Weather Conditions

The optimization of ATI windows design uses typical weather conditions in the US. The conditions include atmospheric temperatures, wind speeds, and solar radiation. Optimization of heat transfer through the inner pane and electric power consumption is performed under different weather conditions.

ATI windows can adapt to different weather conditions. However, they might not completely insulate heat transfer through them at extreme weather conditions.

According to climatic data through 2008, eliminating extremely high temperatures, the average of the highest temperatures in 120 selected cities in the US is $97^{\circ}F$ ($36^{\circ}C$ or $309K$).²⁸ Eliminating extremely low temperatures, the average of the lowest temperatures in 148 selected cities is $7^{\circ}F$ ($-14^{\circ}C$ or $259K$).²⁸ The range of outside temperatures used in the optimization is 7 to $97^{\circ}F$ (-14 to $36^{\circ}C$ or 259 to $309K$).

Eliminating extremely high wind speeds, according to monthly climatic data through 2008 of 111 selected cities in the US, the average maximum wind speed is $21.5m/s$.²⁸ It is used as the highest wind speed, and the lowest is 0.

In clear days, the maximum solar insolation on a surface perpendicular to incoming solar radiation is $1000W/m^2$. This value is used as the highest solar radiation and the lowest is 0.

The indoor temperature is $75^{\circ}F$ ($24^{\circ}C$ or $297K$) and the heat transfer coefficient is $3.6W/m^2$. These are standard testing conditions for windows.²²

To develop a surrogate model by the Response Surface Method to evaluate optimal power supplies under different weather condition within the above ranges, the ATI window design need to be optimized under a set of combinations of weather conditions. The number of weather conditions used here is the small set population size defined by Colaco et al. as equal to ten times the number of variables.²⁹ These sample combinations of weather conditions are generated using Sobol's Quasirandom sequence generator algorithm.³⁰ Thirty sample combinations are generated and are used as weather conditions for the optimization in Section III.B.

III.B. Optimization Models

The design goal of ATI windows is to reduce the heat transfer through the building envelope with the least electric power consumption. It is a multiobjective optimization problem. The objectives of the optimization include both the minimization of the heat exchange between the air inside a room and outside, and the minimization of electric power consumption.

The design variables are what thermostats can control. They are the voltage applied on the TE units, V_{te} , the average pressure gradient of the fans, Δp_{avg} , and the fan pressure gradient slope, k .

The weather conditions, including outside temperatures, T_{out} , wind speeds, v_{wind} , and solar radiation, E_{solar} , are parameters for optimization. The thirty sets of these parameters used in the optimization are generated in Section III.A. For each set of weather condition, optimization is performed and the optimal values of power supplies are evaluated. For different weather conditions, electric powers have different optimal values.

To fit in the channels, the dimensions of the fans should be sufficiently small. Therefore, the average pressure gradient over one fan, Δp_{avg} , and the pressure gradient slope, k , are limited by certain values. The amount of heat transfer is constrained by the operational envelope of the TE units. The dimensions of the side channels limit the number of TE units installed inside them. The conservation of energy through the ATI window system is a necessary equality constraint.

For ATI window, we define two optimization problems, one for cooling conditions and the other for

heating conditions. The one for cooling conditions can be written as

$$\min_x f(x) = w_1 Q_{in}^2 + w_2 P_{TE}^2 \quad (17)$$

$$x = \{V_{te}, \Delta p_{avg}, k\}$$

such that

$$-8 \leq \Delta p_{avg} \leq 8 \quad (18)$$

$$-0.1 \leq k \leq 0.1 \quad (19)$$

$$N_{te} A_{te} \leq A_{channel} \quad (20)$$

$$I_{te} \leq I_{max} \quad (21)$$

$$\Delta T_{te} \leq \Delta T_{max} \quad (22)$$

$$Q_{cold} = Q_{channel} \quad (23)$$

$$Q_{hot} = Q_{hs} \quad (24)$$

Similarly, the optimization for heating conditions is defined as

$$\min_x f(x) = w_1 Q_{in}^2 + w_2 P_{TE}^2 \quad (25)$$

$$x = \{V_{te}, \Delta p_{avg}, k\}$$

such that

$$-8 \leq \Delta p_{avg} \leq 8 \quad (26)$$

$$-0.1 \leq k \leq 0.1 \quad (27)$$

$$N_{te} A_{te} \leq A_{channel} \quad (28)$$

$$I_{te} \leq I_{max} \quad (29)$$

$$\Delta T_{te} \leq \Delta T_{max} \quad (30)$$

$$Q_{hot} = Q_{channel} \quad (31)$$

$$Q_{cold} = Q_{hs} \quad (32)$$

where Q_{in} is the heat transferred through the inner pane; P_{TE} is the electric power consumed by the TE units; w_1 and w_2 are the weights for Q_{in} and P_{TE} ; N_{te} is the number of the TE units; A_{te} is the area of one TE unit installed on the channels; $A_{channel}$ is the available area of the side channels; and $Q_{channel}$ is the heat exchange of the air flow in the channels. The other symbols are defined previously.

Comparing the above two problems for cooling conditions and heating conditions, it can be seen that the only differences are the directions of the heat flow. Eqs. (23) and (24) are constraints for cooling conditions, while Eqs. (31) and (32) are for heating conditions.

III.C. Approximation of Computational Fluid Dynamics Model

The Computational Fluid Dynamics (CFD) model of the ATI window is created in FLUENT to simulate the heat transfer process. Since the computational expense to evaluate the CFD model is high, extended radial basis functions (E-RBF)³¹ are used to develop a response surface based on the results from the CFD analysis. When optimization is performed, at each iteration, a FLUENT simulation is performed to determine the actual heat flux values at some selected points. A trust region is used to establish the valid limits of the response surface.³² The local optimum is achieved based on the local response surface inside the trust region. The new optimum is set as the center for a new neighborhood of points. A new set of points is kept for the surrogate model approximation at the next iteration. The response surface is updated at every iteration and the optimization using the updated surrogate model is performed at the next iteration.

This surrogate model is only used in the approximation of the CFD model; and it is *not* the surrogate model in Sec. IV stored in the thermostat memory.

IV. Surrogate Model of Optimal Operation

Since ATI windows are used under the wide range of weather conditions mentioned in Sec. III.A, they need to adjust the power supplies accordingly to achieve optimal performances. However, the computational

expense of optimization under different weather conditions within the given range is excessive. The Response Surface Method is used to create a surrogate model to approximate optimal power supplies under different weather conditions.

In Section III, the optimization is performed under the thirty combinations of weather conditions. The optimal values of the electric voltage of TE units are used to develop a surrogate model. The optimization results are listed in Table 5. The columns are (1) the weather condition numbers, (2) the outside temperatures, T_{out} , (3) the wind speeds, v_{wind} , (4) the solar radiation, E_{solar} , (5) the optimal voltages of TE units, V_{TE} , (6) the electric power of TE units, P_{TE} , (7) the electric power of fans, P_{fan} , (8) the ratios of electric power consumed by fans to TE units, P_{fan}/P_{TE} , (9) the average pressure gradient over one fan, Δp_{avg} , and (10) the pressure gradient slope, k . The bold outside temperatures are higher than the indoor temperature, $75^\circ F$ ($297K$), and these weather conditions (5, 8, 11, 16, 18, 21, 24, and 28) are cooling conditions.

Table 5. Optimization Results under Selected Weather Conditions

No.	T_{out}		v_{wind}	E_{solar}	V_{TE}	P_{TE}	P_{fan}	$\frac{P_{fan}}{P_{TE}}$	Δp_{avg}	k
	($^\circ F$)	(K)	(m/s)	(W/m^2)	(V)	(W)	(W)	(%)	(Pa)	
1	52	284	10.75	500	1.14	0.97	0.05	5	0.96	0.071
2	74	297	5.38	750	0.97	2.96	0.05	2	0.95	0.067
3	29	272	16.13	250	3.28	9.88	0.09	1	1.77	0.019
4	40	278	8.06	625	1.34	1.17	0.05	4	1.00	0.079
5	85	303	18.81	125	1.00	2.42	0.06	2	1.16	0.069
6	63	290	2.69	375	0.77	0.90	0.05	5	0.97	0.040
7	23	268	6.72	313	3.24	8.71	0.05	1	1.04	0.031
8	91	306	1.34	563	2.48	19.97	0.06	0	1.15	0.051
9	46	281	12.09	63	2.28	6.68	0.07	1	1.53	0.074
10	35	275	4.03	938	2.35	4.49	0.09	2	1.89	0.069
11	80	300	13.78	438	2.37	18.71	0.06	0	1.15	0.079
12	57	287	9.41	188	0.86	0.53	0.02	4	0.46	-0.043
13	12	262	20.16	688	3.20	7.87	0.02	0	0.36	-0.055
14	15	264	10.08	844	2.55	4.59	0.02	0	0.42	-0.047
15	60	289	20.83	344	0.75	0.42	0.03	6	0.57	-0.053
16	82	301	4.70	94	0.97	2.35	0.05	2	0.98	-0.079
17	49	282	2.02	469	1.17	0.96	0.04	5	0.90	-0.072
18	94	307	12.77	969	3.34	37.95	0.06	0	1.17	-0.051
19	26	270	18.14	219	3.28	9.53	0.09	1	1.96	0.066
20	21	267	3.36	531	2.60	5.12	0.08	2	1.61	0.061
21	88	304	8.73	281	1.67	8.95	0.08	1	1.64	0.055
22	43	279	19.48	781	1.49	1.44	0.06	4	1.21	0.079
23	32	273	6.05	156	2.73	6.25	0.06	1	1.27	0.079
24	77	298	16.80	656	0.50	1.00	0.07	7	1.42	0.069
25	54	286	0.67	906	1.34	5.92	0.06	1	1.19	0.067
26	11	261	5.71	609	3.42	9.37	0.13	1	2.63	-0.071
27	56	286	16.46	109	1.45	2.25	0.06	3	1.21	0.042
28	78	299	0.34	359	1.37	6.14	0.08	1	1.75	0.007
29	33	274	11.09	859	1.86	2.47	0.09	4	1.89	0.008
30	44	280	3.02	234	1.84	2.70	0.10	4	2.00	0.015

Based on the data in Table 5, a surrogate model is created using the quadratic response surface method. The inputs of the model are weather condition parameters, including outside temperatures, T_{out} , wind speeds, v_{wind} , and solar radiation, E_{solar} . The ranges of the three inputs are 259 to 309K, 0 to 21.5m/s, and 0 to 1000W/m², respectively. The outputs of the model include the optimal voltages of TE units, V_{TE} ,

the average pressure gradient over one fan, Δp_{avg} , and the pressure gradient slope, k . The three functions are as follows.

$$V_{TE} = a_0 + a_1 T_{out} + a_2 v_{wind} + a_3 E_{solar} + a_{12} T_{out} v_{wind} + a_{13} T_{out} E_{solar} + a_{23} v_{wind} E_{solar} + a_{11} T_{out}^2 + a_{22} v_{wind}^2 + a_{33} E_{solar}^2 \quad (33)$$

$$\Delta p_{avg} = b_0 + b_1 T_{out} + b_2 v_{wind} + b_3 E_{solar} + b_{12} T_{out} v_{wind} + b_{13} T_{out} E_{solar} + b_{23} v_{wind} E_{solar} + b_{11} T_{out}^2 + b_{22} v_{wind}^2 + b_{33} E_{solar}^2 \quad (34)$$

$$k = c_0 + c_1 T_{out} + c_2 v_{wind} + c_3 E_{solar} + c_{12} T_{out} v_{wind} + c_{13} T_{out} E_{solar} + c_{23} v_{wind} E_{solar} + c_{11} T_{out}^2 + c_{22} v_{wind}^2 + c_{33} E_{solar}^2 \quad (35)$$

In the above Eqs. (33), (34) and (35), the a_i 's, b_i 's, and c_i 's, are coefficients determined by the least squares approach using the data in Table 5. The values of the coefficients are listed in Table 6.

Table 6. The Values of the Surrogate Model Coefficients

V_{TE}		Δp_{avg}		k	
a_0	3.05×10^2	b_0	5.67×10	c_0	-7.80
a_1	-2.06	b_1	-3.58×10^{-1}	c_1	5.46×10^{-2}
a_2	4.60×10^{-1}	b_2	-3.31×10^{-1}	c_2	1.33×10^{-2}
a_3	-3.16×10^{-2}	b_3	-6.63×10^{-3}	c_3	-2.61×10^{-4}
a_{12}	-1.40×10^{-3}	b_{12}	1.12×10^{-3}	c_{12}	-5.76×10^{-6}
a_{13}	1.04×10^{-4}	b_{13}	2.23×10^{-5}	c_{13}	1.87×10^{-6}
a_{23}	-5.92×10^{-5}	b_{23}	-4.05×10^{-5}	c_{23}	-1.08×10^{-5}
a_{11}	3.48×10^{-3}	b_{11}	5.76×10^{-4}	c_{11}	-9.64×10^{-5}
a_{22}	-1.82×10^{-3}	b_{22}	5.89×10^{-4}	c_{22}	-2.80×10^{-4}
a_{33}	2.07×10^{-6}	b_{33}	4.33×10^{-7}	c_{33}	-1.47×10^{-7}

In Eqs. (33), (34) and (35), V_{TE} , v_{wind} , and k are functions of three variables, T_{out} , v_{wind} , and E_{solar} . Figures 3, 4 and 5 show the values of the three functions vs one of the variables when the other two variables are fixed at median values.

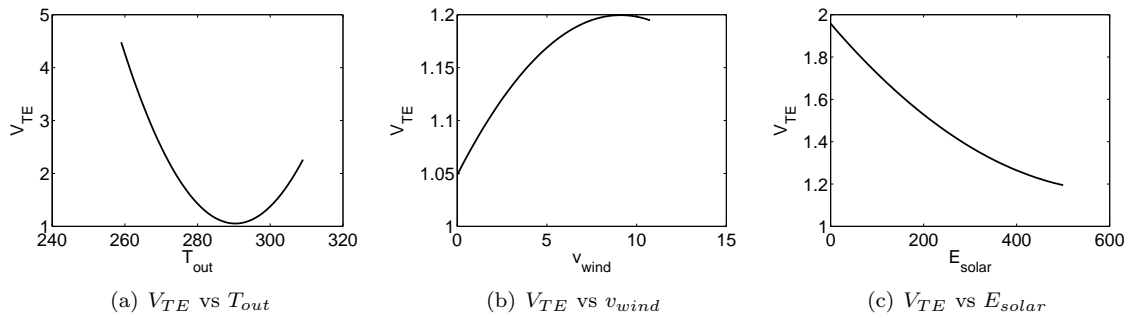


Figure 3. V_{TE} vs the Three Variables T_{out} , v_{wind} , and E_{solar}

The three functions, Eqs. (33), (34) and (35) are stored in the memories of the thermostats. The inputs to the functions, including outside temperatures, T_{out} , wind speeds, v_{wind} , and solar radiation, E_{solar} , are monitored by the sensors described in Sec. II.E. The functions are called by the processor to calculate the optimal electric voltage of the TE units, V_{TE} , the average pressure gradient over one fan, Δp_{avg} , and the pressure gradient slope, k . It is assumed that the weather conditions do not change significantly in a short period of time. Since the conditions are quasi-static, the transitions of inputs and outputs are slow. Transient responses of outputs are not taken into account in this paper.

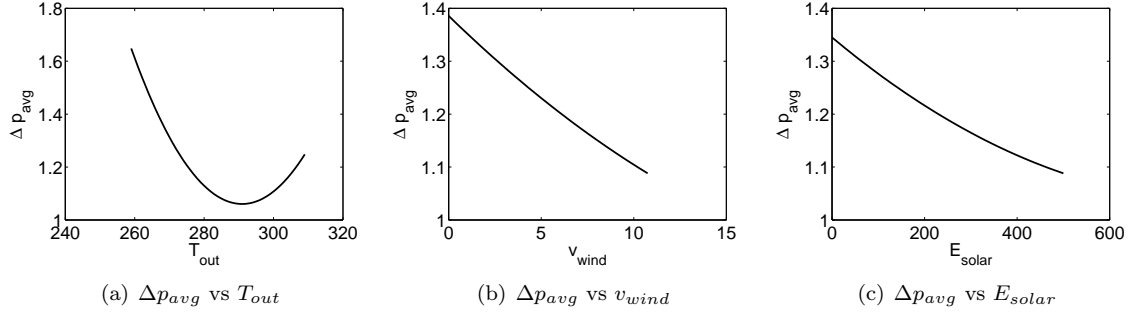


Figure 4. Δp_{avg} vs the Three Variables T_{out} , v_{wind} , and E_{solar}

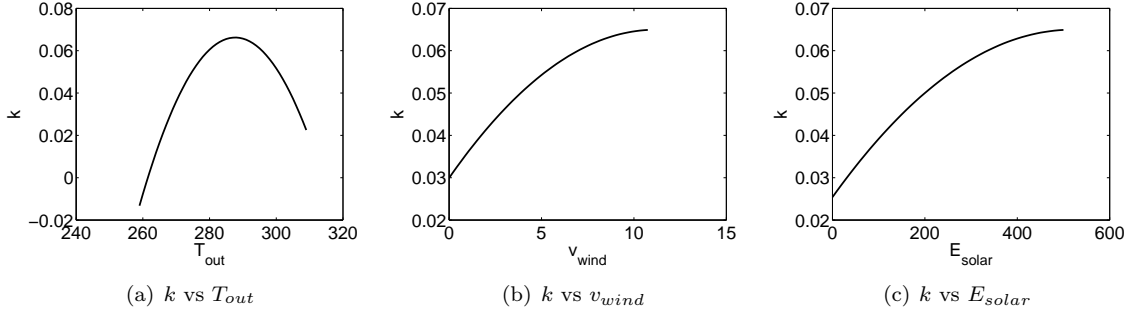


Figure 5. k vs the Three Variables T_{out} , v_{wind} , and E_{solar}

After the calculation of the voltage of the TE units, V_{TE} , TE units power controller adjusts the voltage to the pertinent optimal value.

After the average pressure gradient over one fan, Δp_{avg} , and the pressure gradient slope, k , are evaluated, the pressure gradient of each fan is calculated by the expressions in Table 4. The voltage of each fan is determined by the relation between the voltage and the pressure gradient, which is specified for each fan. This relation is used to determine the values of the voltages of all fans, and fan power controller adjust the voltages to these values.

As the voltage of TE units and the voltages of all fans are adjusted to their optimal values, both the total power supplies and the heat transfer through the inner pane of the ATI windows are optimal under the weather condition.

V. Results and Discussion

ATI windows actively reduce heat transfer through them using electric power consumption, which is very different from traditional windows. The energy efficiency of ATI windows is compared with that of standard HVAC units in this section.

The efficiency of a standard HVAC unit is rated by its Coefficient Of Performance (COP).³³ The COP describes how much heat, Q , can be transferred by a system for a given electrical power input, P . It is generically written as

$$COP = \frac{Q}{P} \quad (36)$$

The COP of an ATI window, COP_{ATI} is defined as how much heat transfer is reduced, compared with a traditional window with the same structure, divided by the electric power used. It is expressed as

$$COP_{ATI} = \frac{Q_{traditional} - Q_{ATI}}{P_{TE}} \quad (37)$$

where $Q_{traditional}$ is the heat transferred through a traditional window; and Q_{ATI} is defined by Eq. (9).

Steady-state energy flow, Q , through a fenestration (such as windows, doors, curtain walls, etc.) can be

written as³⁴

$$Q = UA_{pf}(T_{out} - T_{in}) + (SHGC)A_{pf}E_t \quad (38)$$

where U is an overall coefficient of heat transfer (U-factor); A_{pf} is total projected area of fenestration; SHGC is solar heat gain coefficient; and E_t is incident total irradiance.

A model of a traditional three-pane window is created by *Window*²¹ program. It has the same dimensions and materials as those of the ATI window. The solar heat gain, which is the second part in Eq. (38), is completely determined by the structure of the window. Since the ATI window and the traditional three-pane window have the same structures, the solar heat gain, Q_{solar} , is same for both. The difference of heat transfer through the two kinds of windows is the conductive and convective heat transfer caused by indoor/outdoor temperature difference. For a traditional three-pane window, the conductive and convective heat transfer, Q_{3pane} , is the first part of Eq. (38). It can be written as

$$Q_{3pane} = U_{3pane}A_{pf}(T_{out} - T_{in}) \quad (39)$$

where U_{3pane} is the overall coefficient of heat transfer through a traditional three-pane window.

For the ATI window, it is the heat transfer through the inner pane, Q_{CFD} . The difference of heat transfer between the ATI window and a traditional three-pane window is

$$\Delta Q = Q_{3pane} - Q_{CFD} \quad (40)$$

where U_{3pane} is the overall coefficient of heat transfer through a traditional three-pane window.

From the dimensions in Table 1, A_{pf} of the ATI window or the traditional three-pane window is $1m^2$. Since the heat transfer difference ΔQ is achieved at the expense of electric power supplied to TE units, the COP of ATI windows in Eq. (37) can be written as

$$COP_{ATI} = \frac{\Delta Q}{P_{TE}} \quad (41)$$

The *Window*²¹ program can evaluate U-factors of windows under certain weather conditions. The U-factors of the three-pane window are evaluated by *Window*²¹ program under the weather conditions listed in Table 5, and are substituted into Eq. (40). The COP of the ATI window, COP_{ATI} , is calculated by Eq. (41). The COP values of the ATI window under different weather conditions are listed in Table 7. In Table 7, the values of U_{3pane} , Q_{3pane} , Q_{CFD} and ΔQ are absolute values, and the actual values may be positive or negative according to the directions of heat flow. In this research, if the direction of heat flow is from indoor to outdoor, the actual value is negative; if the direction is from outdoor to indoor, the actual value is positive.

The COP of a standard HVAC system is approximately 3.³³ Figure 6 shows the different values of COP_{ATI} under different weather conditions. The weather condition numbers are from Table 5. It can be seen that, under heating conditions, ATI windows generally have larger COP than the traditional three pane window.

VI. Concluding Remarks

The design optimization of ATI windows illustrates that ATI windows can actively change their overall thermodynamics. The ATI windows are operated at the most appropriate tradeoff between the minimum power consumption and the minimum heat transfer through the windows. The power supplied to TE units, the average pressure gradients of the fans, and the pressure gradient slope of the fans are optimized under selected weather conditions. Based on the optimal results from adaptive optimization, a surrogate model is developed to approximate the optimal operation conditions of the ATI windows as functions of the previous weather conditions. The outside temperatures, wind speeds, and solar radiation, are sensed by thermometers, anemometers, and solar radiation sensors, respectively. The values of these weather signals are used as inputs to the surrogate model, and the optimal values of the power consumption of TE units, the average pressure gradients of the fans, and the pressure gradient slope of the fans are evaluated. Using the surrogate model onsite, the ATI windows are operated optimally under different weather conditions. The comparison of the COP values shows that the ATI window generally has larger values of COP than the traditional three pane window under heating conditions. ATI windows can actively reduce heat transfer through them with efficient use of electric power.

Table 7. COP Values of the ATI Window under Different Weather Conditions

No.	U_{3pane}	Q_{3pane} (W)	Q_{CFD} (W)	ΔQ (W)	P_{TE} (W)	COP_{ATI}
1	1.952	25.38	1.21	26.6	0.97	27.45
2	1.954	0.98	9.08	10.1	2.96	3.40
3	1.942	49.52	3.04	46.5	9.88	4.71
4	1.917	36.90	0.92	37.8	1.17	32.29
5	2.054	11.81	2.74	9.1	2.42	3.74
6	1.852	12.50	1.96	14.5	0.90	16.15
7	1.877	53.73	4.47	49.3	8.71	5.66
8	1.855	16.46	4.72	11.7	19.97	0.59
9	1.953	31.49	1.10	30.4	6.68	4.55
10	1.847	41.33	3.35	44.7	4.49	9.96
11	2.054	5.39	5.13	10.5	18.71	0.56
12	1.955	19.31	1.07	18.2	0.53	34.21
13	1.921	66.99	2.65	64.3	7.87	8.17
14	1.890	62.96	0.55	62.4	4.59	13.60
15	2.005	16.67	0.95	17.6	0.42	42.05
16	1.975	8.27	0.63	7.6	2.35	3.25
17	1.798	26.18	1.39	27.6	0.96	28.79
18	2.054	21.44	5.95	15.5	37.95	0.41
19	1.942	52.55	6.00	46.6	9.53	4.88
20	1.809	54.61	3.54	51.1	5.12	9.97
21	2.018	14.76	1.38	13.4	8.95	1.49
22	1.972	34.88	7.25	42.1	1.44	29.21
23	1.883	45.07	6.71	38.4	6.25	6.13
24	2.054	2.18	10.78	8.6	1.00	8.61
25	1.707	19.52	5.61	25.1	5.92	4.25
26	1.842	65.68	3.68	62.0	9.37	6.62
27	1.985	21.15	0.48	20.7	2.25	9.17
28	1.732	3.19	2.00	1.2	6.14	0.19
29	1.927	44.62	2.37	47.0	2.47	19.02
30	1.835	31.02	1.98	29.0	2.70	10.75

VII. Acknowledgements

Support from the National Found Awards CMMI-0533330, and CMII-0946765 is gratefully acknowledged.

References

- ¹“Table C1A. Total Energy Consumption by Major Fuel for All Buildings, 2003,” Tech. rep., Energy Information Administration, <http://www.eia.doe.gov/emeu/cbecs/>, December 2006.
- ²“Energy Performance Ratings for Windows, Doors, and Skylights,” Tech. rep., Department of Energy, 2005.
- ³Selkowitz, S., Arasteh, D., and Heschong, L., *Residential Windows: A Guide to New Technologies and Energy Performance*, W. W. Norton and Company, 2000.
- ⁴Lee, E. S., Selkowitz, S. E., Levi, M. S., Blanc, S. L., McConahey, E., McClintock, M., Hakkarainen, P., Sbar, N. L., and Myser, M. P., “Active Load Management with Advanced Window Wall Systems: Research and Industry Perspectives,” *Proceedings from the ACEEE 2002 Summer Study on Energy Efficiency in Buildings: Teaming for Efficiency*, Asilomar, Pacific Grove, CA, August 2002.
- ⁵Lee, E. S., DiBartolomeo, D. L., Vine, E. L., and Selkowitz, S. E., “Integrated Performance of an Automated Vene-

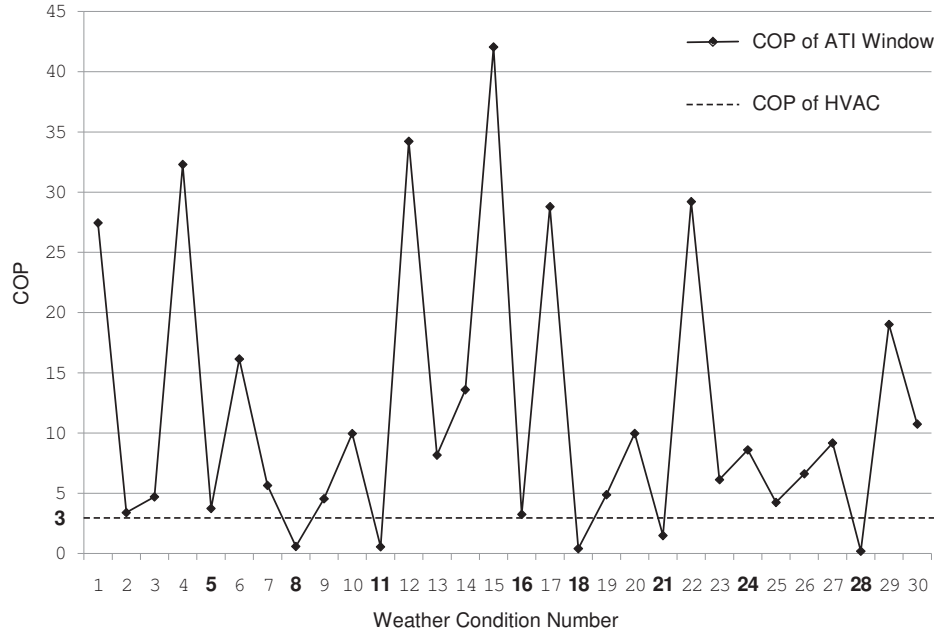


Figure 6. Values of COP_{ATI} under Different Weather Conditions

tian Blind/Electric Lighting System in a Full-Scale Private Office,” *Proceedings of the ASHRAE/DOE/BTECC Conference, Thermal Performance of the Exterior Envelopes of Buildings VII*, Clearwater Beach, FL, December 1998.

⁶Lee, E. S., DiBartolomeo, D. L., and Selkowitz, S. E., “Electrochromic windows for commercial buildings: Monitored results from a full-scale testbed,” *Proceedings from the ACEEE 2002 Summer Study on Energy Efficiency in Buildings: Teaming for Efficiency*, Asilomar, Pacific Grove, CA, August 2002.

⁷Lee, E., Yazdani, M., and Selkowitz, S., “The energy-savings potential of electrochromic windows in the US commercial buildings sector,” Tech. Rep. LBNL-54966, Lawrence Berkeley National Laboratory, <http://repositories.cdlib.org/lbnl/LBNL-54966>, April 2004.

⁸Chow, T., Lin, Z., He, W., Chan, A., and Fong, K., “Use of ventilated solar screen window in warm climate,” *Applied Thermal Engineering*, Vol. 26, No. 14, November 2006, pp. 1910–1918.

⁹Gosselin, J. and Chen, Q., “A computational method for calculating heat transfer and airflow through a dual airflow window,” *Energy and Buildings*, Vol. 40, No. 4, 2008, pp. 452–458.

¹⁰Birchwright, R.-S., Messac, A., Harren-Lewis, T., and Rangavahala, S., “Heat Compensation in Buildings using Thermoelectric Windows: An Energy Efficient Window Technology,” , No. DETC2008-50068, August 2008.

¹¹Messac, A., Birchwright, R.-S., van Dessel, S., Khire, R., and Rangavahala, S., “Optimization-based Design of Active Thermal Insulator: An Energy Efficient Window,” *7th World Congress of Structural and Multidisciplinary Optimization*, Seoul, Korea, May 2007.

¹²Messac, A., Birchright, R.-S., Harren-Lewis, T., and Rangavajhala, S., “Optimizing Thermoelectric Cascades to Increase The Efficiency of Thermoelectric Windows,” *4th AIAA Multidisciplinary Design Optimization Specialist Conference*, Schaumburg, IL, April 2008.

¹³Harren-Lewis, T., Messac, A., Zhang, J., and Rangavajhala, S., “Multidisciplinary Design Optimization of Energy Efficient Side-Channel Windows,” *5th AIAA Multidisciplinary Design Optimization Specialist Conference*, AIAA, Palm Springs, CA, May 2009.

¹⁴Rowe, D. M., *Thermoelectrics Handbook: Macro to Nano*, CRC PrI LIC, 2006.

¹⁵Jha, A. K. and Kudva, J. N., “Morphing aircraft concepts, classifications, and challenges,” *Proc. SPIE: Smart Structures and Materials 2004: Industrial and Commercial Applications of Smart Structures Technologies*, Vol. 5388, July 2004, pp. 213–224.

¹⁶Wlezién, R. W., Horner, G. C., McGowan, A. R., Padula, S. L., Scott, M. A., Silcox, R. J., and Simpson, J. O., “Aircraft Morphing program,” *Proc. SPIE: Smart Structures and Materials 1998: Industrial and Commercial Applications of Smart Structures Technologies*, Vol. 3326, June 1998, p. 176C187.

¹⁷Janah, M., “Changing Gears,” *Red Herring*, August 2000, pp. 230C232.

¹⁸Webb, A., “A piston revolution,” *Engineering Management Journal*, February 2002, pp. 25C30.

¹⁹Box, G. E. and Draper, N. R., “Empirical Model-building and Response Surface,” *John Wiley and Sons, Inc.*, 1987.

²⁰Melcor, *Melcor Thermoelectric Handbook*, <http://www.melcor.com/handbook.html>, 2007.

²¹Lawrence Berkeley National Laboratory, University of California, *WINDOW 6.2 / THERM 6.2 Research Version User Manual*, January 2008.

- ²²Mitchel, R., Kohler, C., Arasteh, D., Carmody, J., Huizeng, C., and Curcija, D., "Therm 5/Windows NFRC Simulation Manual," Tech. rep., Lawrence Berkeley National Laboratory, June 2003.
- ²³Fluent Inc., Lebanon, NH, *FLUENT 6.3 User's Guide*, September 2006.
- ²⁴Carli, Inc., Amherst, MA, *TARCOG: Mathematical Models For Calculation Of Thermal Performance Of Glazing Systems With Or Without Shading Devices*, October 2006.
- ²⁵Incropera, F. P., Dewitt, D. P., Bergman, T. L., and Lavine, A. S., *Introduction to Heat Transfer*, John Wiley & Sons, 5th ed., 2007.
- ²⁶Stanescu, G., Fowler, A. J., and Bejan, A., "The optimal spacing of cylinders in free-stream cross-flow forced convection," *International Journal of Heat and Mass Transfer*, Vol. 39, No. 2, 1996, pp. 311–317.
- ²⁷"Fans - Efficiency and Power Consumption," Tech. rep., <http://www.engineeringtoolbox.com>.
- ²⁸"Comparative Climatic Data for the United States through 2008," Tech. rep., <http://www.noaa.gov>.
- ²⁹J., C. M., S., D. G., and D., S., "A response surface method-based hybrid optimizer," *Inverse Probl Sci Eng*, Vol. 6, No. 16, 2008, pp. 717–741.
- ³⁰Sobol, I. M., "Uniformly Distributed Sequences with an Additional Uniform Property," *USSR Computational Mathematics and Mathematical Physics*, Vol. 16, 1976, pp. 236–242.
- ³¹Mullur, A. A. and Messac, A., "Extended radial basis functions: more flexible and effective metamodeling," *AIAA Journal*, Vol. 43, No. 6, 2005, pp. 1306–1315.
- ³²Lewis, R. M., "A trust region framework for managing approximation models in engineering optimization," *6th AIAA/NASA/ISSMO Symposium on Multidisciplinary Analysis and Optimization*, 1996, pp. 1053–1055.
- ³³"ENERGY STAR Program Requirements for Light Commercial HVAC," Tech. rep., <http://www.energystar.gov>.
- ³⁴"2009 ASHRAE Handbook - Fundamentals (I-P Edition)," Tech. rep., American Society of Heating, Refrigerating and Air-Conditioning Engineers, Inc., 2009.